SANDIA REPORT
SAND2009-3812
Unlimited Release
Printed June 2009

Wall pressure exerted by hydrogenation of sodium aluminum hydride

Daniel E. Dedrick, Yon E. Perras, Mark D. Zimmerman

Prepared by
Sandia National Laboratories
Albuquerque, New Mexico 87185 and Livermore, California 94550

Sandia is a multiprogram laboratory operated by Sandia Corporation,
a Lockheed Martin Company, for the United States Department of Energy's
National Nuclear Security Administration under Contract DE-AC04-94AL85000.

Issued by Sandia National Laboratories, operated for the United States Department of Energy by Sandia Corporation.

Available to DOE and DOE contractors from
U.S. Department of Energy
Office of Scientific and Technical Information
P.O. Box 62
Oak Ridge, TN 37831

Telephone: (865) 576-8401
Facsimile: (865) 576-5728
E-Mail: reports@adonis.osti.gov
Online ordering: http://www.osti.gov/bridge

Available to the public from
U.S. Department of Commerce
National Technical Information Service
5285 Port Royal Rd.
Springfield, VA 22161

Telephone: (800) 553-6847
Facsimile: (703) 605-6900
E-Mail: orders@ntis.fedworld.gov
Online order: http://www.ntis.gov/help/ordermethods.asp?loc=7-4-0#online

SAND2009-3812
Unlimited Release
Printed Month Year

Wall pressure exerted by hydrogenation of sodium aluminum hydride

Daniel E. Dedrick, Mark D. Zimmerman, Yon E. Perras
Thermal/Fluid Science and Engineering
Sandia National Laboratories
P.O. Box 969
Livermore, California 94551-MS9409

Abstract

Wall pressure exerted by the bulk expansion of a sodium aluminum hydride bed was measured as a function of hydrogen content. A custom apparatus was designed and loaded with sodium alanates at densities of 1.0, 1.1, and 1.16 g/cc. Four complete cycles were performed to identify variations in measured pressure. Results indicated poor correlation between exerted pressure and hydrogen capacity of the sodium alanate beds. Mechanical pressure due to the hydrogenation of sodium alanates does not influence full-scale system designs as it falls within common design factors of safety. Gas pressure gradients within the porous solid were identified and may limit reaction rates, especially for high aspect ratio beds.

ACKNOWLEDGMENTS

The authors wish to acknowledge the program support from General Motors Research and Development, specifically the support and contribution of Jim Spearot, Director of Chemical and Environmental Sciences Laboratory at the General Motors Research and Development Center.

CONTENTS

FIGURES

NOMENCLATURE

με	micro strain in units of change in length over length
DOE	Department of Energy
SNL	Sandia National Laboratories

1. INTRODUCTION

Pressure due to expansion of a storage material during hydrogen sorption is a classic metal hydride system safety issue. This pressure originates from expansion of the crystal structure during hydrogen sorption and can be exacerbated by a physical process called decrepitation. Decrepitation is the systematic physical breakdown of larger particles into smaller fines due to high strain induced by hydrogen cycling [1]. Following decrepitation, the fines tend to settle under the influence of gravity and/or vibration, thus causing density gradients to form. Upon subsequent cycling, these high density sections of the bed expand. Due to a lack of void space in the region, the expansion is directed outward, exerting large forces on the wall of the containment vessel. In extreme cases, structural failures of the containment vessel can occur, causing a release of hydrogen gas and exposure of the reactive storage materials to the surrounding environment. The hydride containment vessel must withstand the hydrogen gas pressure and the mechanical pressure exerted by bulk material expansion. The summation of these two pressures dictates the strength characteristics of the containment structure.

Each hydrogen sorption material will behave differently with respect to expansion forces. Some materials will not establish large density gradients due to sintering, while others will experience significant decrepitation events with just a few cycles. This property disparity requires systems designers to characterize each material as a function of sorption cycle by monitoring the stain in the containment vessel wall. Nasako and colleagues have described methods for measuring stress and strain in a hydride-containing vessel wall [4]. The strain measurement of a hydride-containing vessel wall can be difficult for two reasons; 1) the temperature excursions intrinsic to the uptake and release of hydrogen can cause significant strain measurement errors, and 2) the strain induced by the gas pressure can complicate the measurement of the mechanical expansion induced strain. In practice, these difficulties can be overcome with clever instrumentation including temperature compensation and gas pressure induced signal calibration.

1.1 Sodium alanates

The complex metal hydrides, such as sodium alanates, have also been considered for hydrogen storage systems. Like conventional metal hydrides, sodium alanates expand and contract during the sorption of hydrogen. The single crystal density of stoichiometric sodium alanates decreases by 33% during hydrogenation - shown in the mixture below.

MIXTURE A

2.17 g/cc		2.02 g/cc		1.46 g/cc
100 NaH + 100 Al +4Ti + 12 NaCl	⇔	$33Na_3AlH_6$ + 66Al +4Ti + 12 NaCl	⇔	100NaAlH4 + 4Ti + 12 NaCl

Sodium alanate compositions that are more appropriate for full-scale systems may contain non-stoichiometric amounts of excess aluminum [1], which alters the weighted single crystal density. The following non-stoichiometric mixture is of specific interest for full-scale systems where the single crystal density decreases by 29% during hydrogenation:

MIXTURE B

2.23 g/cc		2.09 g/cc		1.59 g/cc
100 NaH + 127Al + 4Ti + 12 NaCl	⇔	$33Na_3AlH_6$ + 93Al +4Ti + 12 NaCl	⇔	100NaAlH4 + 27Al + 4Ti + 12 NaCl

Previous mechanical wall pressure measurements of Mixture A have been completed with some

success [2]. Results at 1.0 g/cc packing density were found to exert negligible pressure up to capacities of 3.3 wt%. Packing densities of 1.2 g/cc have been shown to cause significant pressure (~1000 psi), high flow restriction, along with unfavorable sorption characteristics. High hydraulic pressures (>10 ksi) were required to pack the un-hydrided powder into the test cell at 1.2 g/cc. These previous measurements lacked direct calibration and temperature compensation which adversely affected the measurement accuracy.

Following these initial measurements, Mixture B was chosen due to improved sorption and thermal properties. Hydrogen capacities exceeding 3.8 wt% were routinely achieved and higher packing densities are attainable due to the increase in aluminum content [1]. Due to the significant differences in performance between Mixture A and Mixture B, additional wall pressure measurements were undertaken.

2. APPARATUS

New hardware was developed to overcome key limitations in the first generation of experiments reported at the 2004 ASM conference [2]. By maintaining the sample in cylindrical geometry and measuring the radial expansion force, the new geometry more closely imitated full scale bed designs. Temperature compensation was added to the pressure sensing circuit, and direct calibration capabilities were integrated. A complete description of the strain gauge circuit is described in the Appendix.

The measurement apparatus consisted of two parts; the hydrogen pressure vessel and the expansion force sensing vessel. The hydrogen pressure vessel allows for in-situ cycling of the hydrogen storage material and consists of a heating/cooling jacket and electronics feed though. The expansion force sensing vessel senses the bulk expansion without the influence of the gas pressure by maintaining equal gas pressure on each side of the sensing element.

The expansion force sensing vessel is an open-ended 304 series stainless steel cylinder with a 0.030 inch wall thickness. The dynamic pressure range of this sensor is ~1200psi limited by plastic failure of the pressure-sensitive cylinder at 1300με. Two transducer quality strain gauges were affixed to the surface of the cylinder – see Appendix A for more information. Axial expansion of the material is limited by an aluminum structure (see Figure 1). The sensing vessel is capped on each end by a PTFE spacer that functions to provide a physical and thermal barrier between the hydrogen storage material and the surrounding components. Tolerances were designed into the structure to accommodate thermal expansion of all materials and to maintain the sensing vessel in a normally unconstrained state.

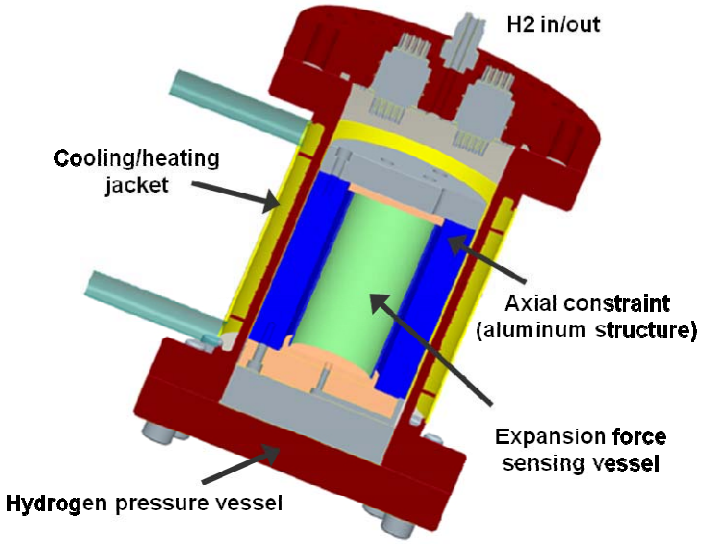

Figure 1. Experimental hardware developed for the expansion force measurements included an external hydrogen pressure vessel and an internal force sensing vessel

4. CALIBRATION

Rigorous and direct calibration methodologies are required to ensure the greatest pressure-measurement accuracy. A direct gas pressure calibration method was designed to characterize each of the sensing vessels. The method was performed externally of the hydrogen pressure vessel, using aluminum caps with o-ring seals. Pressure relief was integrated to avoid compromising the structural integrity of the cylinder. Helium was added to the system through a manifold and a correlation of pressure and strain was generated. This calibration was completed at various temperatures to capture the effect of variable strength and modulus of elasticity of the stainless steel.

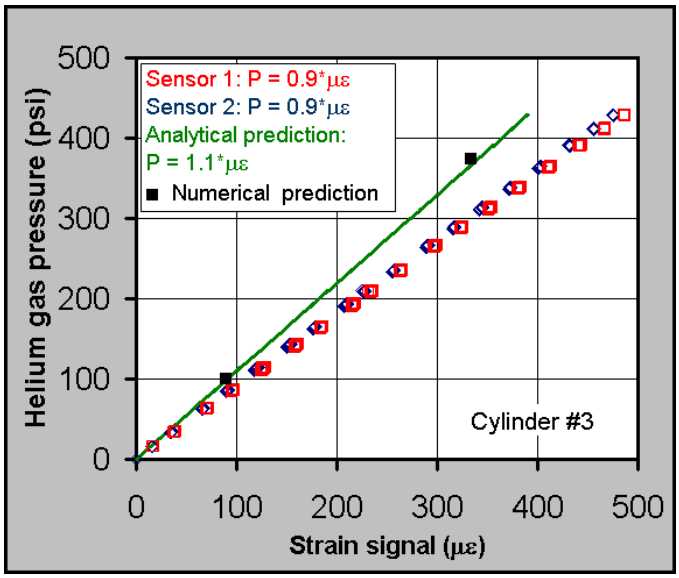

Figure 2. Example of direct calibration of expansion force sensing vessel. The pressure response is highly linear.

Three total sensing vessels were calibrated during these experiments, each with a pressure response of 0.9 psi/με (amplifier output ~220 psi/V). Analytic and numerical calculations predict a pressure response of 1.1 psi/με. The difference between prediction and actual measurements (as shown in Figure 2) may be due to physical properties estimation error of the cylinder, gauge miss-alignment, and/or strain sensing error caused by the bonding process; however, this becomes less important due to direct calibration.

4.1 Temperature Compensation

The strain gauge circuit includes temperature compensation by including the “zero” strain direction gauge in the Wheatstone bridge (described in the Appendix). Any residual temperature response not addressed electronically in the Wheatstone bridge was characterized during external calibration. For cylinder #3 shown in Figure 2, eleven total temperature response tests were performed. The existence of the residual temperature response is likely due to elemental differences in wires or contact resistances. The magnitude of the response usually falls near 0.6±0.125 με/K (0.5 psi/K). This temperature response is removed from the strain signal using a temperature measurement.

4.2 Error discussion

Direct calibration eliminates the following sources of error:

- sensor placement/miss-alignment with the axial and radial direction.
- inaccurate material properties estimation
- inaccurate vessel dimensions (thickness and diameter)
- un-compensated lead resistance

Sources of measurement error include:

- Amplifier balance/calibration - The balance and calibration process is accurate to within 1 με
- Temperature response - Temperature variation is kept below 40K during testing – this would result in a signal error of 5 με at 0.125 με/K temperature response error
- Amplifier drift - Maximum drift rate observed was 0.2 με/hr. Measurements are completed within 24 hours providing a maximum drift of 4.8με
- Calibration gas pressure measurement (especially below 100psi) - This error is negligible due to the calibration record of the pressure transducer and the linear response of the sensing vessel (Figure 2)
- Lead resistance changes - These variations are not accounted for due to minimal environmental changes and small temperature response of the lead wire material (Cu).

Additional errors are present due to gas flow resistance and/or thermal expansion. This causes a transient pressure signal that is not specifically correlated to the hydrogen uptake/release of the hydride material. This is discussed in greater detail within the *Results* section. Results from this error analysis indicate that all measurements are accurate within < 11 με (12 psi).

5. RESULTS

Measurements of Mixture B were completed at 1.0, 1.1, and 1.16 g/cc. Since the results from each density are strikingly similar, the results discussion will only focus on data from the 1.16 g/cc sample.

The first two absorption tests of any sample yields a complex pressure signal that is difficult to correlate to any specific and physical process (see cycles 1 - 2 in Figure 3). The appearance of this behavior is repeatable between samples, although it is not well understood. The author speculates that strain is introduced to the pressure sensor during loading of the alanate precursors. This strain is then relieved during the first few sorption cycles and does not re-appear. Regardless of the cause, the perceived pressure experienced is on order of 100 psi – a small quantity compared to the gas pressures present. The absorption cycles following the initial activation are largely un-interesting with pressure signals on order of the system error (12 psi).

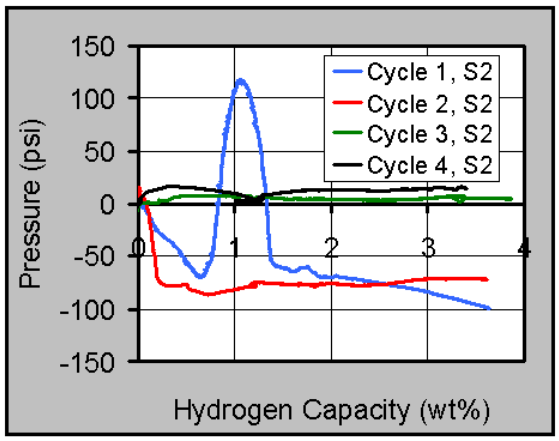

Figure 3 - Pressure sensed during cycles 1 - 4 demonstrates that the sample initially relaxes, then exerts minimal pressure during absorption

Due to the lack of strain caused by absorption, pressure release during decomposition was not expected. As predicted, no real or perceived pressure was experienced during the decomposition of the sodium aluminum tetrahydride ($NaAlH_4$) phase. Interestingly, as the system is heated for the decomposition of sodium aluminum hexahydride phase (Na_3AlH_6), a steady increase of pressure up to ~250 psi is experienced. This perceived pressure decreases as the reaction nears completion (see Figure 4). Subsequent heating of a decomposed bed does not result in any pressure as shown in Figure 5. It is likely that the pressure developed during desorption is due to the thermal expansion of the sodium aluminum hexahydride phase. It is not likely that this signal is due to a pressure differential in the bed since the measured pressure exceeds the equilibrium pressure in the bed.

That being said, some gas pressure gradients are present within the bed – especially during the first 1 wt% of decomposition. Figure 6 describes the typical pressure experienced during decomposition as a function of gauge position and hydrogen evolved. The pressure sensor in the center of the bed experiences up to 300 psi higher pressure than the sensor near the edge. No gas pressure gradients between the two sensors are observed after the first 10 minutes of decomposition.

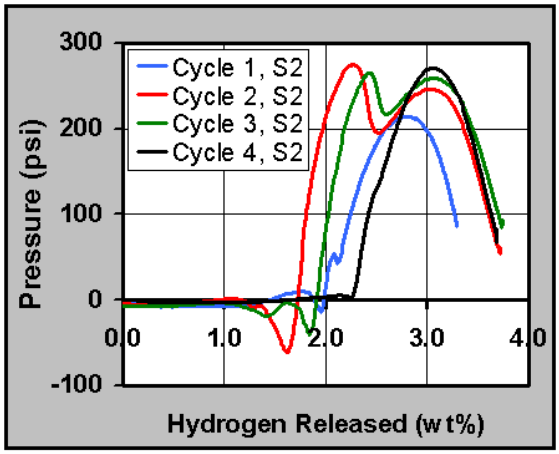

Figure 4. Decomposition of the tetrahydride phase exerts minimal pressure. Up to 250psi of pressure is exerted, possibly due to thermal expansion.

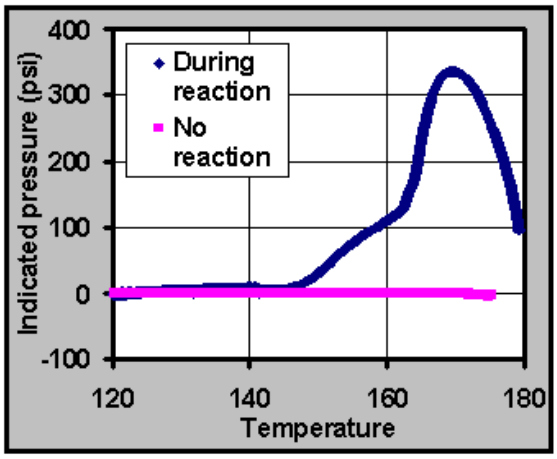

Figure 5. Pressure due to hydride heating is only observed during decomposition of the hexahydride phase. Heating of the decomposed bed does not result in a pressure signal.

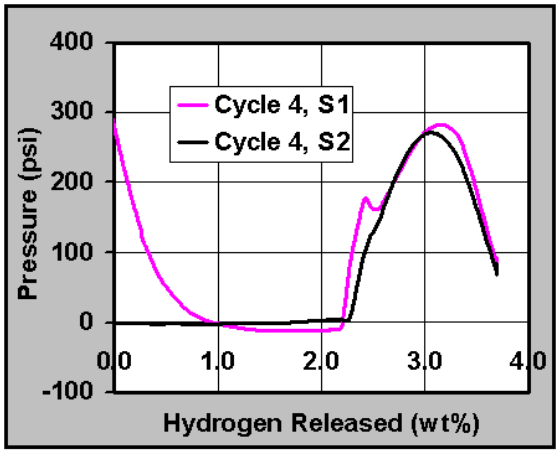

Figure 6. Gas pressure gradients are present within the bed during the first 10 minutes (1 wt%) of desorption. "S1" represents the gauge near the mid-point of the bed (high pressure) while "S2" is placed near the edge (low pressure).

3. CONCLUSIONS

There is no significant correlation between exerted pressure and hydrogen capacity of sodium alanate beds. Mechanical pressure due to the hydrogenation of sodium alanates does not influence the full-scale system design although gas pressure gradients within the material may limit reaction rates, especially for high aspect ratio beds. We recommend monitoring strain in large-scale systems during operation to verify that trends do not change over many cycles. Other compositions, chemistries, and geometries should be analyzed individually as necessary.

4. REFERENCES

1. US Patent Pending 20070178042, 'Sodium Alanate Hydrogen Storage Material'
2. D. Dedrick, *Engineering Properties of Complex Hydrides for System Optimization* ASM Materials Solutions Conference, Columbus, OH (2004)
3. B. Fultz / Journal of Alloys and Compounds; 14 March 2002; vol.335, p.165-75
4. K. Nasako / Journal of Alloys and Compounds 264 (1998) 271–276

APPENDIX: STRAIN GAGE INSTALLATION METHODS

This memo describes the techniques used to properly acquire strain measurements on a cylindrical stainless steel tube as it applies to a particular experiment. It should be noted that some of the techniques used in this application may not be the most effective for all situations.

Figure 1 below shows the actual physical mounting of the two strain gages mounted to the .030" stainless steel tube. An adhesive called M-Bond 610, manufactured by Vishay was used to bond the gages to the tube. M-Bond 610 is recommended for applications where temperatures go as high as 230 degrees C. Application notes are available from Vishay (Instruction Bulletin B-130) and they describe the techniques used to correctly bond the transducers.

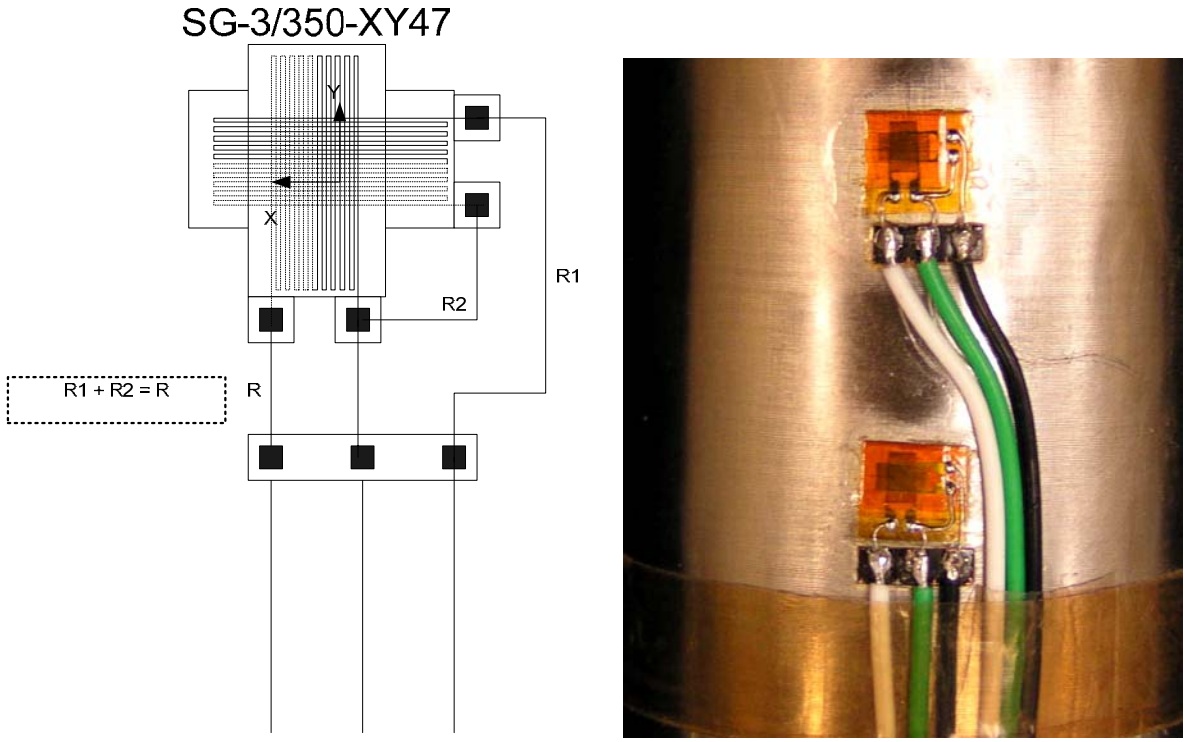

Figure 7. Bi-axial strain Gage Setup

In this particular application, two bi-axial strain gauges were acquired from Omega Engineering. Bi-axial units were chosen over uniaxial ones, since a compensating gauge was needed to cancel the effect of thermal output. Temperature compensation is essential if one is to accurately measure strain since it can be on the order of 0.5 /^{o}K. For this particular test case, the temperature increase will be at 200 ^{o}K and could theoretically account for errors as high as a 100 . This thermal error can be substantial on test specimens with low average strain measurements and may be lost in the noise if special attention is not given to the setup.

One of the 2 gauges will be used as a "dummy gauge" or simply a resistor, since it forms one of the arms in the Wheatstone bridge. The active gauge, sees exactly the same temperature changes and thus the same thermal resistance changes. If the adjacent arms have the same resistance

value, including the leads, then no bridge unbalance is present and the two outputs cancel. The only output that will be created by the bridge unbalance is generated by the strain in the one of the axes of the test specimen. It is important that no strain exist in the "dummy" axis.

The illustration to left shows the electrical diagram with the resistance assignments. The solder pad was added for strain relief. The values R1, R2 and R are resistance values of the short lead wires connected to the solder pad. The resistance value of R should be equal to the sum of R1 and R2. This is accomplished by making the corresponding lead wires out of the same gauge wire, with equivalent lengths. The picture shows that, in this case, that R will be slightly less than the sum of R1 and R2. This difference is extremely small and should not create any substantial errors.

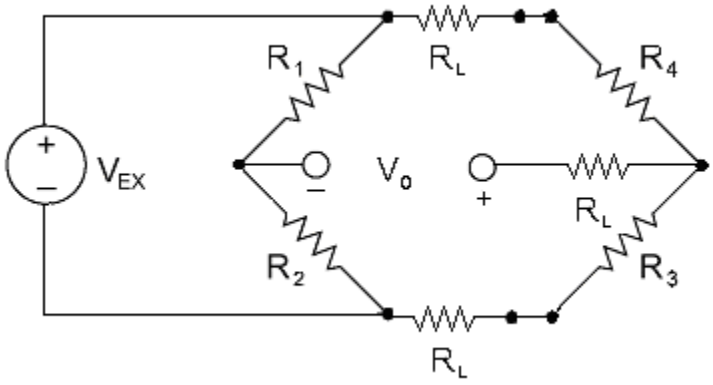

Figure 8. Wheatstone Bridge Circuit

Figure 2 shows a typical Wheatstone bridge circuit, where:

V_{EX} = excitation voltage
V_o = Bridge output voltage
R_1 & R_2 = bridge completion resistances
R_3 & R_4 = strain gages (350)
R_L = lead wire resistance

If the lead resistance is the same in each arm, R_L is a constant and the above equation can be written as:

$$V_O = \left[\frac{R_3}{R_3 + R_4} - \frac{R_2}{R_1 + R_2}\right] \bullet V_{EX}$$

If all lead resistance values are not the same, then by examining the voltage divider equation above it can be seen how the bridge can become unbalanced and lead to erroneous strain measurements.

From the equation above, it becomes apparent that when all resistances are equal, the output signal is zero. In the temperature compensated setup, R_3 becomes the active gage and R_4 becomes the "dummy" gauge. Any changes in temperature will cause the resistance to change

equally for both gauges, thus keeping the balance in the bridge. When a strain is applied, the unbalance will generate a voltage which is proportional only to the strain.

Figure 3 shows the lead wires attached to the feed-through connector and the corresponding lead wires that eventually go to a Vishay 2120B amplifier system. It is important that the wires be routed close to each other, forcing them to be at the same temperature. This allows each arm in the bridge to maintain the canceling effect due to equal resistance changes in adjacent arms.

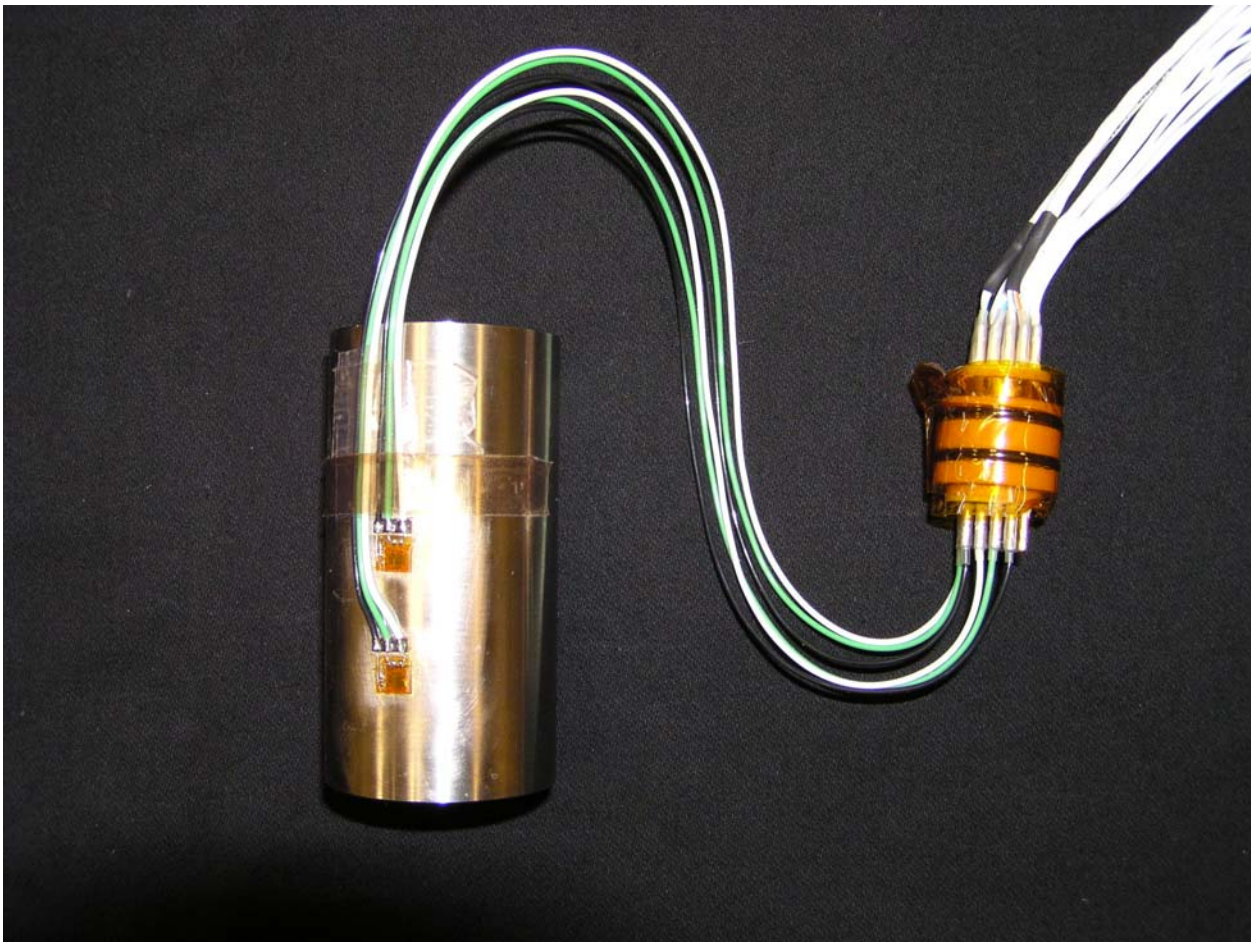

Figure 9. Test specimen assembly

Omega Strain Gauge (SG-3/350-XY47) Specifications are as follows.

- Gauge Factor = 2.07
- Date of Manufacture: 2/26/04
- Batch Number: MO2348
- C.H.T. = 769
- Resistance = 350 +/- 0.5%
- Constantan Foil with temperature coefficient matched to Stainless Steel
- Gage Dimension: 3.0 mm Tall by 2.8 mm wide

DISTRIBUTION

2	MS9018	Central Technical Files	8944
2	MS0899	Technical Library	4536